NASA/TM—2001-211122

Thermal Conductivity of Ceramic Thermal Barrier and Environmental Barrier Coating Materials

Dongming Zhu
Ohio Aerospace Institute, Brook Park, Ohio

Narottam P. Bansal
Glenn Research Center, Cleveland, Ohio

Kang N. Lee
Cleveland State University, Cleveland, Ohio

Robert A. Miller
Glenn Research Center, Cleveland, Ohio

September 2001

The NASA STI Program Office . . . in Profile

Since its founding, NASA has been dedicated to the advancement of aeronautics and space science. The NASA Scientific and Technical Information (STI) Program Office plays a key part in helping NASA maintain this important role.

The NASA STI Program Office is operated by Langley Research Center, the Lead Center for NASA's scientific and technical information. The NASA STI Program Office provides access to the NASA STI Database, the largest collection of aeronautical and space science STI in the world. The Program Office is also NASA's institutional mechanism for disseminating the results of its research and development activities. These results are published by NASA in the NASA STI Report Series, which includes the following report types:

- TECHNICAL PUBLICATION. Reports of completed research or a major significant phase of research that present the results of NASA programs and include extensive data or theoretical analysis. Includes compilations of significant scientific and technical data and information deemed to be of continuing reference value. NASA's counterpart of peer-reviewed formal professional papers but has less stringent limitations on manuscript length and extent of graphic presentations.

- TECHNICAL MEMORANDUM. Scientific and technical findings that are preliminary or of specialized interest, e.g., quick release reports, working papers, and bibliographies that contain minimal annotation. Does not contain extensive analysis.

- CONTRACTOR REPORT. Scientific and technical findings by NASA-sponsored contractors and grantees.

- CONFERENCE PUBLICATION. Collected papers from scientific and technical conferences, symposia, seminars, or other meetings sponsored or cosponsored by NASA.

- SPECIAL PUBLICATION. Scientific, technical, or historical information from NASA programs, projects, and missions, often concerned with subjects having substantial public interest.

- TECHNICAL TRANSLATION. English-language translations of foreign scientific and technical material pertinent to NASA's mission.

Specialized services that complement the STI Program Office's diverse offerings include creating custom thesauri, building customized data bases, organizing and publishing research results . . . even providing videos.

For more information about the NASA STI Program Office, see the following:

- Access the NASA STI Program Home Page at ***http://www.sti.nasa.gov***

- E-mail your question via the Internet to help@sti.nasa.gov

- Fax your question to the NASA Access Help Desk at 301–621–0134

- Telephone the NASA Access Help Desk at 301–621–0390

- Write to:
  NASA Access Help Desk
  NASA Center for AeroSpace Information
  7121 Standard Drive
  Hanover, MD 21076

NASA/TM—2001-211122

Thermal Conductivity of Ceramic Thermal Barrier and Environmental Barrier Coating Materials

Dongming Zhu
Ohio Aerospace Institute, Brook Park, Ohio

Narottam P. Bansal
Glenn Research Center, Cleveland, Ohio

Kang N. Lee
Cleveland State University, Cleveland, Ohio

Robert A. Miller
Glenn Research Center, Cleveland, Ohio

National Aeronautics and
Space Administration

Glenn Research Center

September 2001

Acknowledgments

This work was supported by NASA Ultra-Efficient Engine Technology (UEET) Program. The authors are grateful to George W. Leissler at NASA Glenn Research Center for his assistance in the preparation of plasma-sprayed TBC and EBC coatings specimens. Thanks are due to John Setlock for his help with hot pressing of various ceramic compositions.

Available from

NASA Center for Aerospace Information
7121 Standard Drive
Hanover, MD 21076

National Technical Information Service
5285 Port Royal Road
Springfield, VA 22100

Available electronically at http://gltrs.grc.nasa.gov/GLTRS

THERMAL CONDUCTIVITY OF CERAMIC THERMAL BARRIER AND ENVIRONMENTAL BARRIER COATING MATERIALS

Dongming Zhu, Narottam P. Bansal, Kang N. Lee and Robert A. Miller
National Aeronautics and Space Administration
Glenn Research Center
Cleveland, Ohio 44135

ABSTRACT

Thermal barrier and environmental barrier coatings (TBCs and EBC's) have been developed to protect metallic and Si-based ceramic components in gas turbine engines from high temperature attack. Zirconia-yttria based oxides and $(Ba,Sr)Al_2Si_2O_8$ (BSAS)/mullite based silicates have been used as the coating materials. In this study, thermal conductivity values of zirconia-yttria- and BSAS/mullite-based coating materials were determined at high temperatures using a steady-state laser heat flux technique. During the laser conductivity test, the specimen surface was heated by delivering uniformly distributed heat flux from a high power laser. One-dimensional steady-state heating was achieved by using thin disk specimen configuration (25.4 mm diam and 2 to 4 mm thickness) and the appropriate backside air-cooling. The temperature gradient across the specimen thickness was carefully measured by two surface and backside pyrometers. The thermal conductivity values were thus determined as a function of temperature based on the 1-D heat transfer equation. The radiation heat loss and laser absorption corrections of the materials were considered in the conductivity measurements. The effects of specimen porosity and sintering on measured conductivity values were also evaluated.

INTRODUCTION

Environmental barrier coatings (EBC's) have been developed to protect Si-based ceramic components in gas turbine engines from high temperature environmental attack [1–3]. With continuously increasing demands for significantly higher engine operating temperature, fuel efficiency and better engine reliability, future EBC systems must be designed for both thermal and environmental protections of the engine components in gas turbine combustion gas environment [4]. In particular, thermal barrier functions of EBC's become a necessity for reducing the engine component thermal loads and chemical reaction rates, thus maintaining required mechanical properties and durability of these components. The development of advanced thermal barrier and environmental barrier coatings (TBC's and EBC's) will directly impact the successful use of ceramic components in advanced engine systems.

Plasma-sprayed ZrO_2-8 wt% Y_2O_3, and $(Ba,Sr)Al_2Si_2O_8$(BSAS)-mullite coatings have been successfully used as thermal barrier coatings for superalloy components, and environmental barrier coatings for SiC/SiC ceramic matrix composite (CMC) systems, respectively. In this study, a laser steady-state heat flux technique is established to evaluate high temperature thermal conductivity of both the hot-pressed and plasma-sprayed TBC/EBC materials. The thermal conductivity data are of great importance for future advanced coating design.

MATERIALS AND EXPERIMENTAL METHODS

Materials

Several TBC and EBC coating materials, including ZrO_2-8 wt% Y_2O_3, BSAS, mullite, and mullite+BSAS mixtures, were tested at high temperatures to determine their thermal conductivity values using a laser steady state heat flux test technique. The test specimens were either hot-pressed disks (25.4 mm diam and 2 to 4 mm thickness), or 254 to 400-μm thick plasma-sprayed coatings. The hot-pressed specimens were fabricated using spray-dried powders at 1500 °C for an hour under 30 MPa pressure. The coating specimens were prepared by plasma-spraying the powders onto superalloy disks (25.4 mm diam and 3.2 mm thickness) or on melt-infiltrated (MI) SiC/SiC ceramic matrix composites (25.4 mm diam and 2.2 mm thickness) substrates.

Thermal Conductivity Testing

Thermal conductivity testing of the ceramic coating materials was carried out using a 3.0 kW CO_2 laser (wavelength 10.6 μm) high-heat flux rig. A schematic diagram of the test rig and photos of the actual test facilities are illustrated in Fig. 1, and the general test approaches have been described elsewhere [5–9]. In this steady-state laser heat flux thermal conductivity test, the specimen surface heating was provided by the laser beam, and backside air-cooling was used to maintain the desired specimen temperatures. A uniform laser heat flux was obtained over the 23.9 mm diam aperture region of the specimen surface by using an integrating ZnSe lens combined with the specimen rotation. Platinum wire flat coils (wire diam 0.38 mm) were used to form thin air gaps between the top aluminum aperture plate and stainless-steel back plate to minimize the specimen heat losses through the fixture.

The thermal conductivity $k_{ceramic}$ of the ceramic materials can be determined from the pass-through heat flux q_{thru} and measured temperature difference $\Delta T_{ceramic}$ across the ceramic specimen (or the ceramic coating) thickness $l_{ceramic}$ under the steady-state laser heating conditions [5, 7]

$$k_{ceramic} = q_{thru} \cdot l_{ceramic} / \Delta T_{ceramic} \tag{1}$$

The actual pass-through heat flux q_{thru} for a given ceramic specimen was obtained by subtracting the laser reflection loss (measured by a 10 μm reflectometer) and the calculated radiation heat loss (total emissivity was taken as 0.50 for the oxides and silicates) at the ceramic coating surface (i.e., $q_{thru} = q_{delivered} - q_{reflected} - q_{radiated}$) from the laser delivered heat flux. Note that the non-reflected laser energy is assumed to be absorbed at or near the specimen surfaces because of the quite high emissivity at the 10.6 μm laser wavelength region for the oxides and silicates. In some test cases, the pass-through heat flux q_{thru} was verified with an internal heat flux gauge incorporated with the substrates (instrumented specimens) via an embedded miniature thermocouple. For the hot pressed bulk specimens, the temperature

difference $\Delta T_{ceramic}$ in the ceramic was directly measured by using surface and backside pyrometers (both 8 μm infrared pyrometers, emissivity was set at 0.94 for ZrO_2-Y_2O_3 oxides, and at 0.97 for mullite and BSAS silicates). For the coating specimens, the temperature difference in the ceramic coating $\Delta T_{ceramic}$ was obtained from the measured coating surface and substrate backside temperatures using an 8 um pyrometer and a two-color pyrometer, respectively, and subtracting the temperature drops in the substrate and bond coat

$$\Delta T_{ceramic} = T_{ceramic-surafce} - T_{substrate-back} - \int_0^{l_{bond}} \frac{q_{thru} \cdot dl}{k_{bond}(T)} - \int_0^{l_{substrate}} \frac{q_{thru} \cdot dl}{k_{substrate}(T)} \qquad (2)$$

where $T_{ceramic-surafce}$ and $T_{substrate-back}$ are measured ceramic surface and substrate backside temperatures, l_{bond}, $l_{substrate}$, and $k_{bond}(T)$ and $k_{substrate}(T)$ are the thicknesses and the temperature-dependent thermal conductivity of the bond coat and substrate, respectively.

RESULTS AND DISCUSSION

Phase Structures of Coating Materials

Figure 2 shows the typical X-ray diffraction results of ZrO_2-8 wt% Y_2O_3, BSAS, and BSAS+mullite materials. The plasma-sprayed and hot-pressed ZrO_2-8 wt% Y_2O_3 had a tetragonal t' phase with some monoclinic and cubic phases after the processing and the laser thermal conductivity testing. However, more monoclinic and cubic phases were usually present in the hot-pressed ZrO_2-8 wt% Y_2O_3 specimen probably due to the lower processing temperature. Both hot-pressed and plasma-sprayed BSAS specimens showed mainly the $(Ba,Sr)Al_2Si_2O_8$ celsian phase. The BSAS+mullite mixture specimen contained both the $(Ba,Sr)Al_2Si_2O_8$ celsian and mullite phases, as expected.

Thermal Conductivity of ZrO_2-8 wt% Y_2O_3

ZrO_2-8 wt% Y_2O_3 (ZrO_2-4.55 mol%) is extensively used as the thermal barrier coating material because of its low thermal conductivity and excellent mechanical properties. The thermal conductivity of a hot-pressed specimen as a function of test temperature is shown in Fig. 3 (a). The dense bulk material had a conductivity value of 2.0 to 2.3 W/m-K, and showed only slight temperature dependence.

The thermal conductivity of a 180-μm thick, plasma-sprayed ZrO_2-8 wt% Y_2O_3 coating specimen on a nickel based superalloy substrate as a function of time is shown in Fig. 3 (b). The relatively porous, microcracked thermal barrier coating (with 10 vol% porosity) was tested at a surface temperature of 1316 °C for 20 hr. It can be seen that the coating had an initial conductivity value of 1.0 W/m-K, but after 20 hr laser testing the conductivity increased to 1.4 W/m-K due to the ceramic sintering.

Thermal Conductivity of BSAS and Mullite

Figure 4 shows the thermal conductivity test results of a hot-pressed BSAS disk specimen using the laser heat flux technique. The measured thermal conductivity of this specimen was about 2.8 to 3.0 W/m-K in the temperature range of 800 to 1400 °C. A sudden drop in conductivity during the heating cycle is due to possible specimen cracking. The conductivity results are consistent with the conductivity measurements of a laser sintered, 254-μm thick dense BSAS coating specimen on a nickel base superalloy substrate (Fig. 5). From Fig. 5, it can also be seen that thermal conductivity of a 254-μm thick plasma-sprayed mullite coating showed stronger temperature dependence than BSAS. Lower conductivity values were measured at high temperature regime. The mullite coating had conductivity values of ~1.9 to 2.5 W/m-K in the temperature range of 1000 to 1400 °C.

For the as plasma-sprayed BSAS coating, the initial conductivity values can be significantly lower due to the presence of higher porosity. As shown in Fig. 6, the initial thermal conductivity of BSAS was about 1.4 W/m-K at 900 °C. Considerable conductivity increase was observed during the first heating-cooling cycle due to the ceramic sintering. After the first test cycle, the conductivity increased to ~2.2 W/m-K at 900 °C.

Thermal Conductivity of BSAS and Mullite Mixtures

Figure 7 shows the thermal conductivity test results of hot-pressed BSAS and mullite mixture disk specimens using the laser heat flux technique. The measured thermal conductivity values for the two materials were about 3.0 W/m-K at 600 °C and 1.6 to 2.0 W/m-K at 1500 °C. A slightly higher conductivity was observed for the higher BSAS containing (30 wt% BSAS+70mullite) material.

Similar to the plasma sprayed BSAS coating, the plasma-sprayed BSAS + mullite mixture coatings also showed lower initial conductivity value due to porosity. As shown in Fig. 8, the 254-μm thick mullite+20 wt% BSAS coating had an initial conductivity of 1.5 W/m-K, and increased to 2.0 W/m-K at 900 °C after the first heating cycle due to sintering. However, the coating had less conductivity increase due to sintering as compared to pure BSAS coating.

Thermal Conductivity of TBC/EBC Systems

Thermal conductivity of TBC/EBC systems was also investigated. Fig. 9 shows the thermal conductivity test results of a two-layer BSAS/mullite+20 wt% BSAS coating that was coated on the SiC/SiC CMC substrate. The first heating-cooling cycle had a significant conductivity increase due to the larger initial ceramic sintering. The second heating-cooling cycle, however, showed much less conductivity increase. This is because at the given test temperatures, most of the sintering and densification had occurred during the first cycle.

In order to evaluate multilayer TBC/EBC coating conductivity information at high temperature, a ZrO_2-8 wt% Y_2O_3/mullite/Si/SiC-SiC CMC system was tested at a surface temperature of 1560 °C with a laser pass-thru heat flux of 115 W/m-K. Figure 10 (a) and (b) show the coating thermal conductivity, and the estimated temperature distribution across the coating system. The overall initial ceramic coating conductivity was about 1.6 to 1.8 W/m-K, but the conductivity quickly increased to about 2.2 W/m-K after the high temperature exposure for a short period of time. A slight decrease in coating conductivity may be related to some microcracking of the coating systems. Coating sintering and delamination will become important issues for developing advanced ceramic coating systems designed for high temperature and high thermal gradient applications.

CONCLUSIONS

A laser steady-state heat flux technique has been used to investigate thermal conductivity of several TBC and EBC coating materials. Thermal conductivity values of the current BSAS and mullite based EBC coating materials were in the range of 1.9 to 3.0 W/m-K, as compared to ~2.0 W/m-K for the ZrO_2-8 wt% Y_2O_3 thermal barrier coating material. The plasma-sprayed coatings showed lower initial conductivity values (1.4 W/m-K for EBCs and 1.0 W/m-K for ZrO_2-8 wt% Y_2O_3) as compared to the hot oppressed bulk coating materials due to higher porosity. Significant conductivity increase was observed for the plasma-sprayed TBC and EBC coating systems after the laser high temperature thermal exposure because of ceramic sintering and densification.

REFERENCES

[1] K.N. Lee and R.A. Miller, "Development and Environmental Durability of Mullite and Mullite/YSZ Dual Layer Coatings for SiC and Si_3N_4 Ceramics," *Surface and Coatings Technology*, vol. 86–87, pp. 142–148, 1996.

[2] K.N. Lee, "Key Durability Issues with Mullite-Based Environmental Barrier Coatings for Si-Base Ceramics," *Transactions of the ASME*, vol. 122, pp. 632–636, 2000.

[3] K.N. Lee, "Current Status of Environmental Barrier Coatings for Si-Based Ceramics," *Surface and Coatings Technology*, vol. 133–134, pp. 1–7, 2000.

[4] D. Zhu, K.N. Lee, and R.A. Miller, "Thermal Conductivity and Thermal Gradient Cyclic Behavior of Refractory Silicate Coatings on SiC/SiC Ceramic Matrix Composites," NASA TM–210824, NASA Glenn Research Center, Cleveland, April 2001.

[5] D. Zhu and R.A. Miller, "Thermal Conductivity and Elastic Modulus Evolution of Thermal Barrier Coatings Under High Heat Flux Conditions," NASA TM–209069, NASA Glenn Research Center, Cleveland, Ohio, April 1999.

[6] D. Zhu and R.A. Miller, "Thermal Conductivity and Elastic Modulus Evolution of Thermal Barrier Coatings Under High Heat Flux Conditions," *Journal of Thermal Spray Technology*, vol. 9, pp. 175–180, 2000.

[7] D. Zhu and R.A. Miller, "Thermal Conductivity Change Kinetics of Ceramic Thermal Barrier Coatings Determined by the Steady-State Laser Heat Flux Technique," NASA Glenn Research Center, Cleveland, Ohio, NASA TM–209639, Research and Technology 1999, pp. 29–31, March 2000.

[8] D. Zhu and R.A. Miller, "Thermal Barrier Coatings for Advanced Gas-Turbine Engines," *MRS Bulletin*, vol. 27, pp. 43–47, 2000.

[9] D. Zhu, R.A. Miller, B.A. Nagaraj, and R.W. Bruce, "Thermal Conductivity of EB-PVD Thermal Barrier Coatings Evaluated by a Steady-State Laser Heat Flux Technique," *Surface and Coatings Technology*, vol. 138, pp. 1–8, 2001.

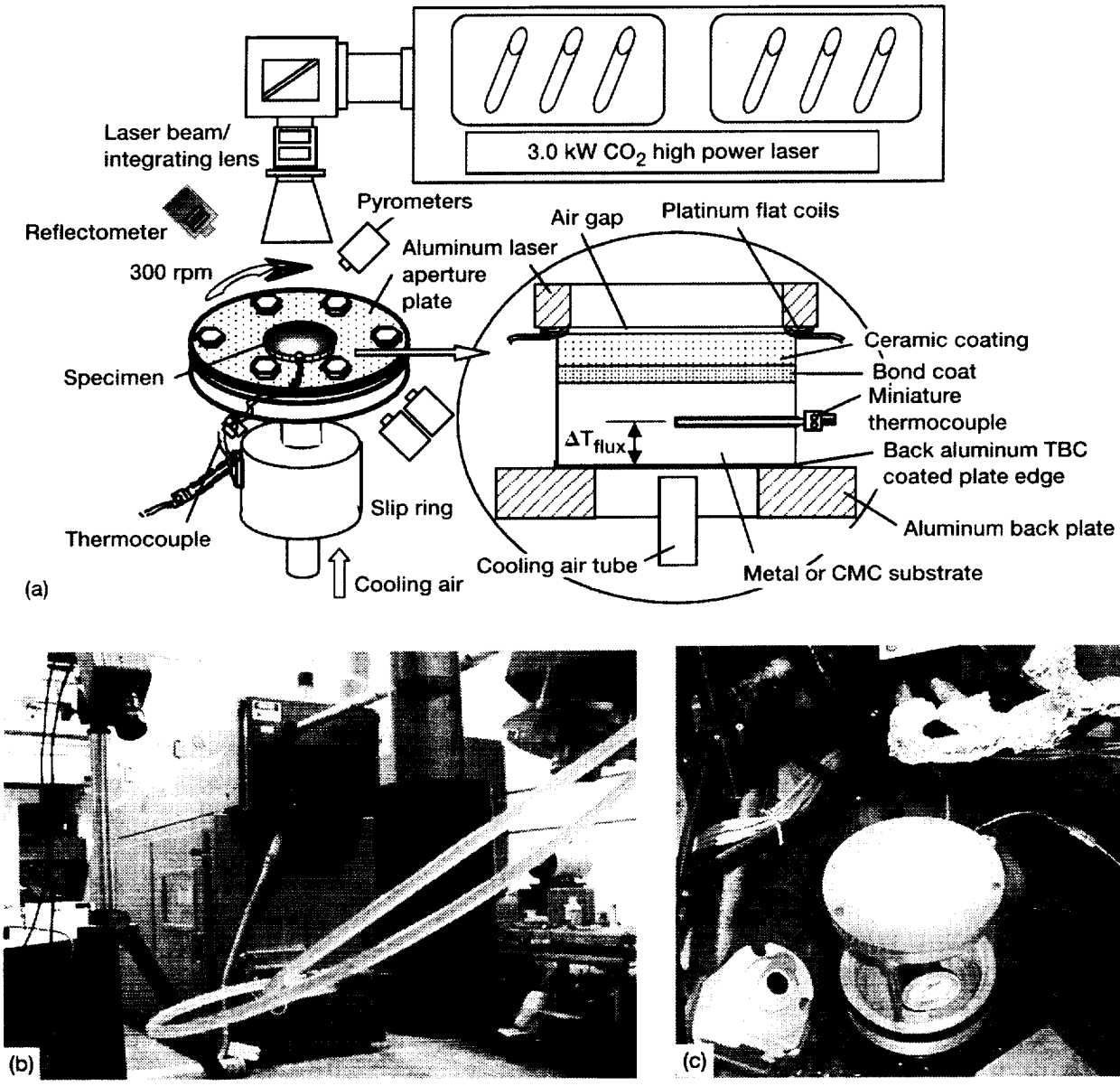

Figure 1.—Laser high heat flux rig for determining thermal conductivity of TBC/EBC materials. During the test, the ceramic surface and the substrate backside temperatures are measured by infrared pyrometers. The thermal conductivity of the ceramics can be determined from the pass-through heat flux and measured temperature difference through the ceramic specimen (or the ceramic coating) thickness under the steady-state laser heating conditions by a one-dimensional (one-D) heat transfer model. (a) Schematic diagram laser test rig; (b) A 3.0 kW CO_2 continuous wave laser system; (c) The test rig with a ceramic specimen under testing.

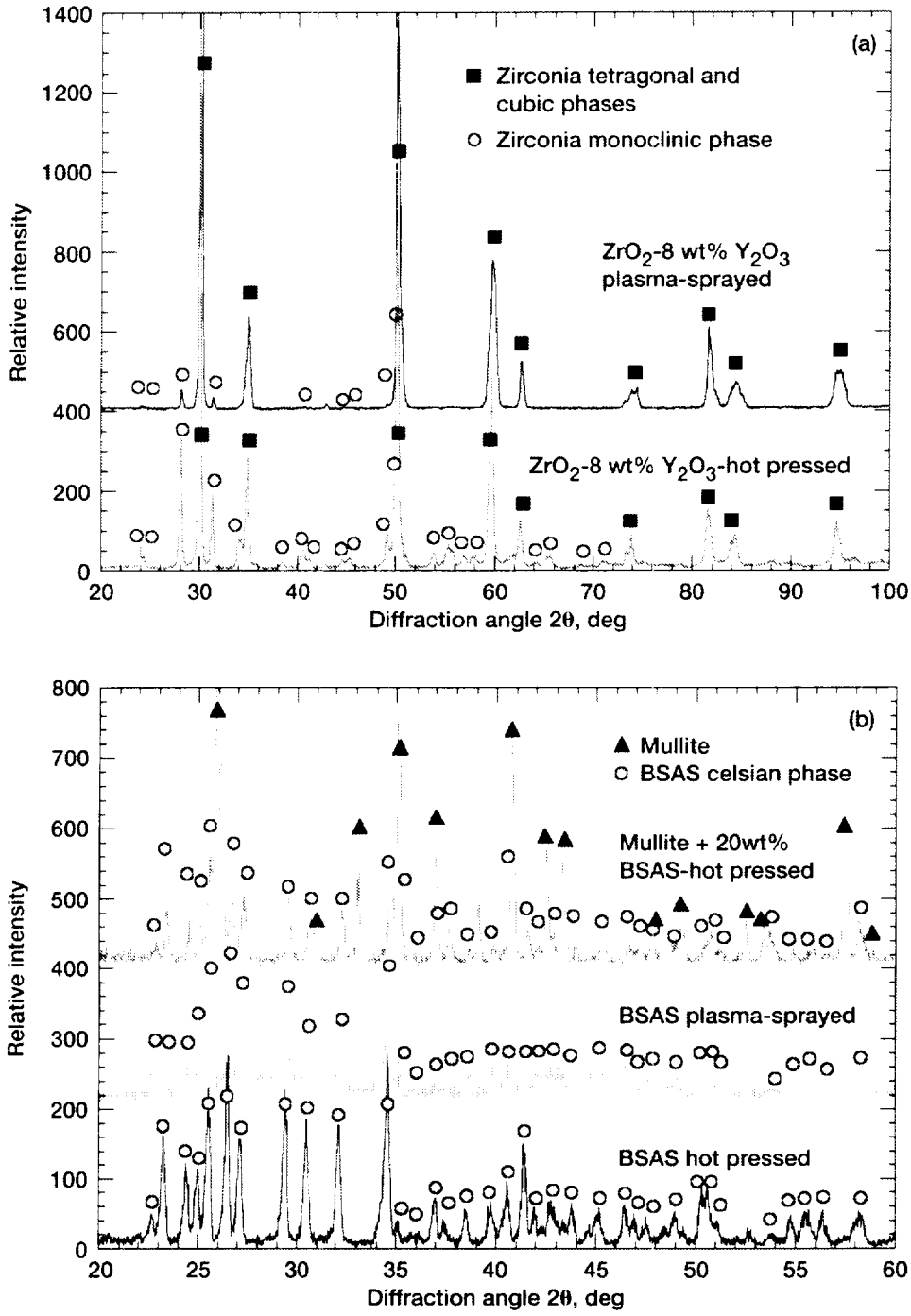

Figure 2.—Typical X-ray diffraction patterns of (a) ZrO_2-8 wt% Y_2O_3, and (b) BSAS, and BSAS + mullite materials.

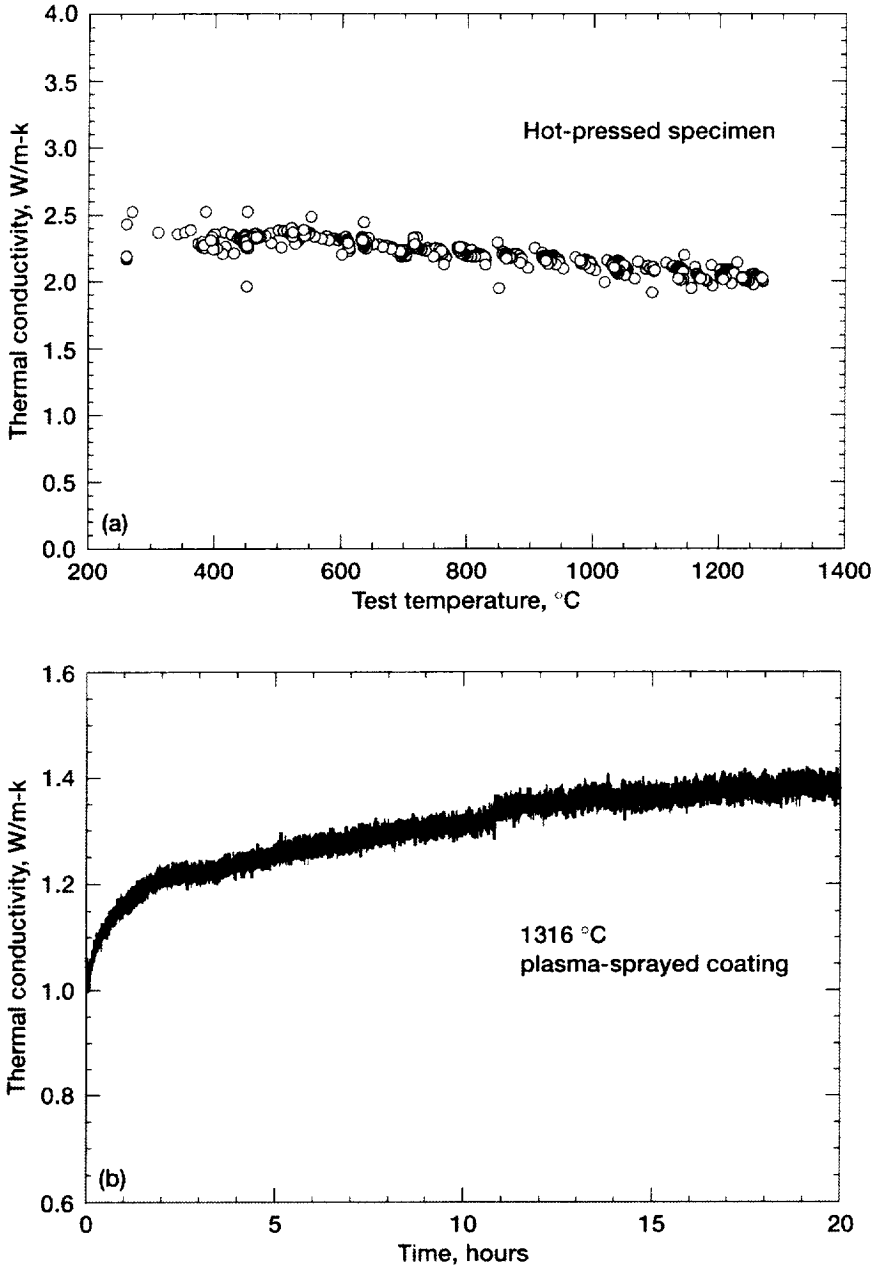

Figure 3.—Thermal conductivity of ZrO_2-8 wt% Y_2O_3 determined by steady-state laser heat flux technique. (a) Thermal conductivity of a hot pressed specimen as a function of temperature. (b) Thermal conductivity of a plasma-sprayed coating specimen as a function of test time at 1316 °C.

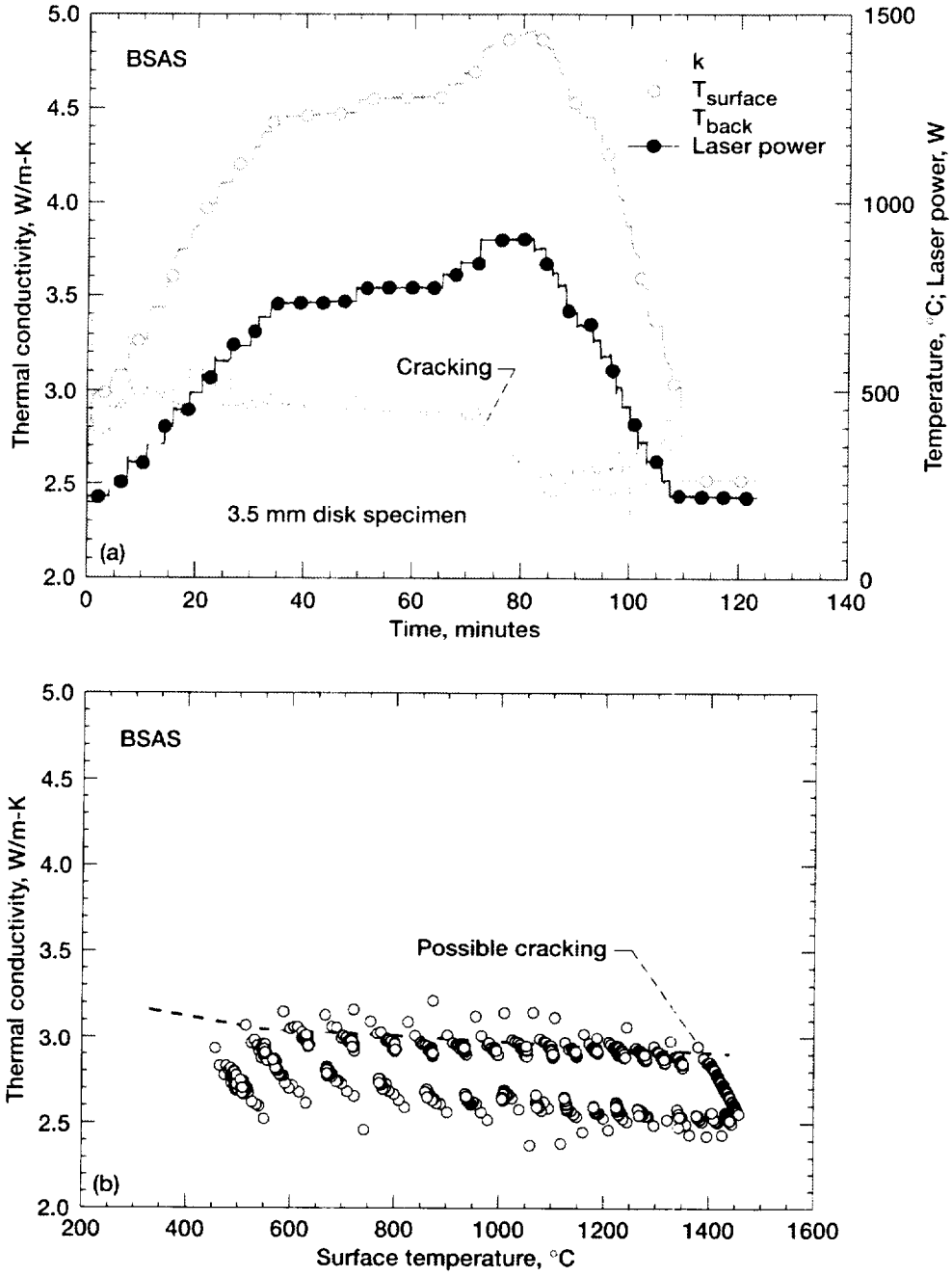

Figure 4.—Thermal conductivity k of a hot-pressed BSAS specimen determined from a steady-state laser test technique. (a) Thermal conductivity of BSAS specimen as a function of test time during a heat-cooling cycle. A sudden drop in conductivity during heating is due to possible specimen cracking. (b) Thermal conductivity of BSAS specimen as a function of surface test temperature (the dashed line indicates the average ceramic thermal conductivity).

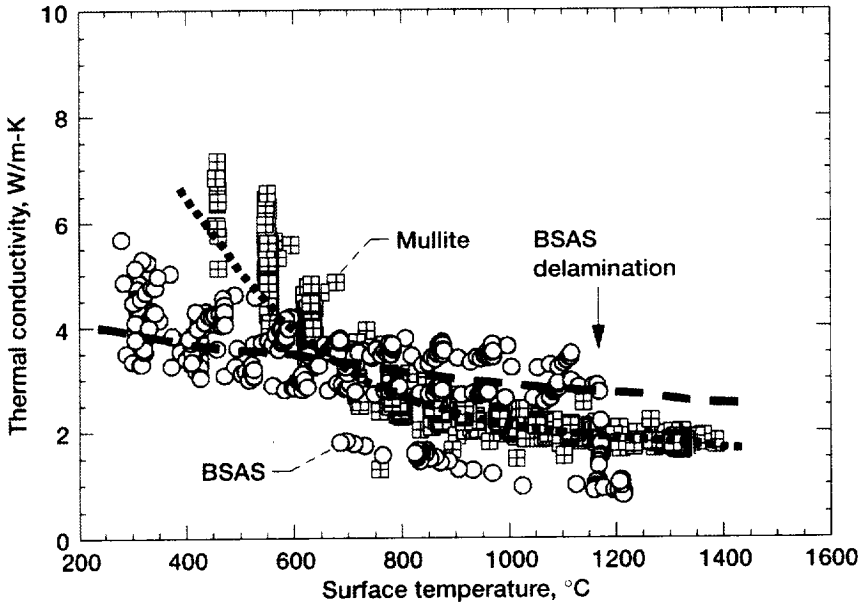

Figure 5.—Thermal conductivity of 254 μm thick, plasma-sprayed BSAS and mullite coatings on superalloy substrate specimens. The coating specimens were previously laser-sintered at 1300 °C for 2 hours and thermal conductivity of the coating specimens were measured using a heating-cooling cycle (the dashed lines represent estimated average thermal conductivity values).

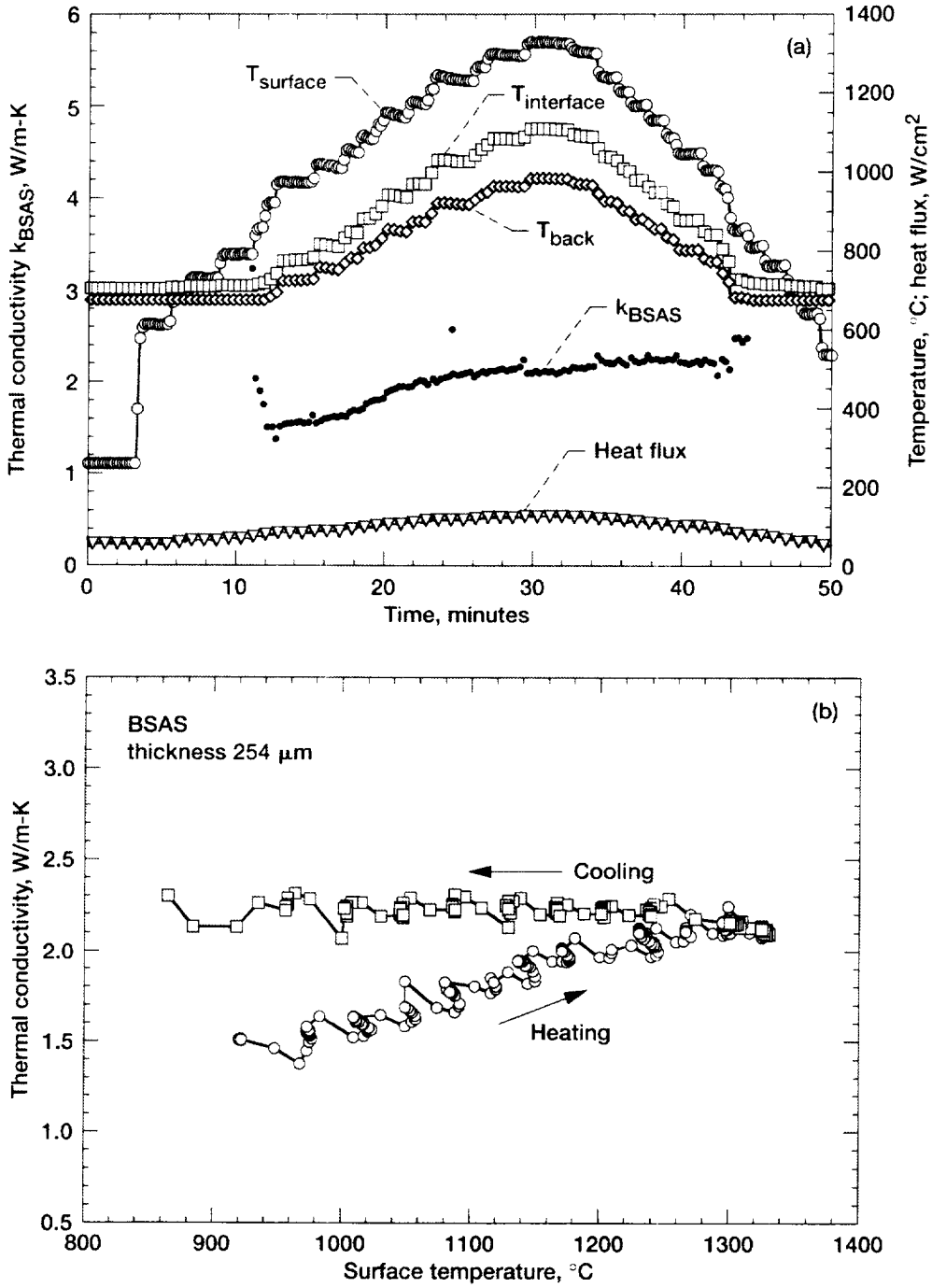

Figure 6.—Thermal conductivity of 254 μm thick, plasma-sprayed BSAS coating on SiC/SiC CMC substrate. (a) Thermal conductivity of BSAS coating as a function of test time during a heat-cooling cycle. The conductivity rise is due to the coating sintering. (b) Thermal conductivity of BSAS coating as a function of test temperature.

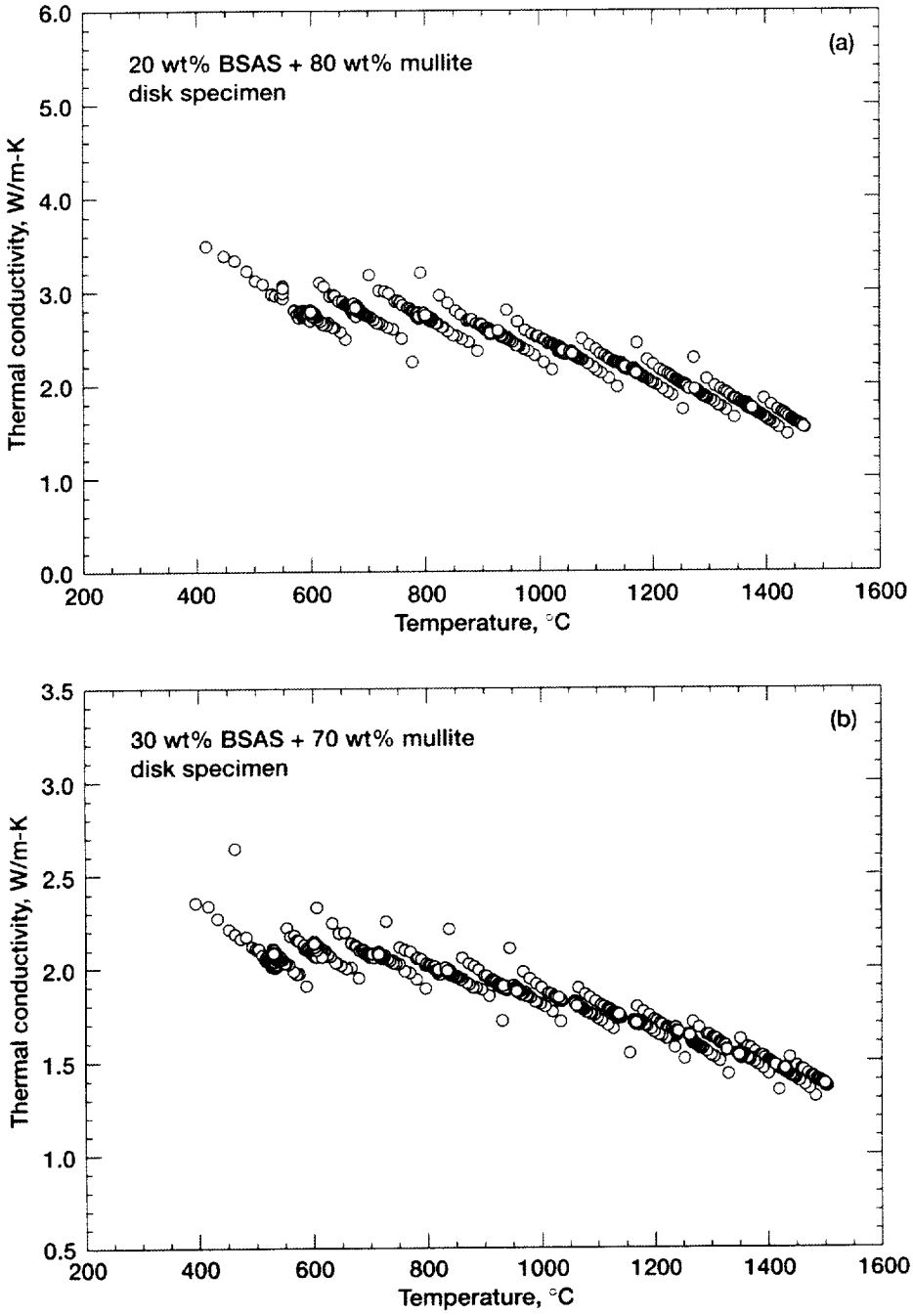

Figure 7.—Thermal conductivity of hot-pressed BSAS and mullite mixture disk specimens as a function of test temperature. (a) Mullite-20 wt% BSAS; (b) Mullite + 30 wt% BSAS.

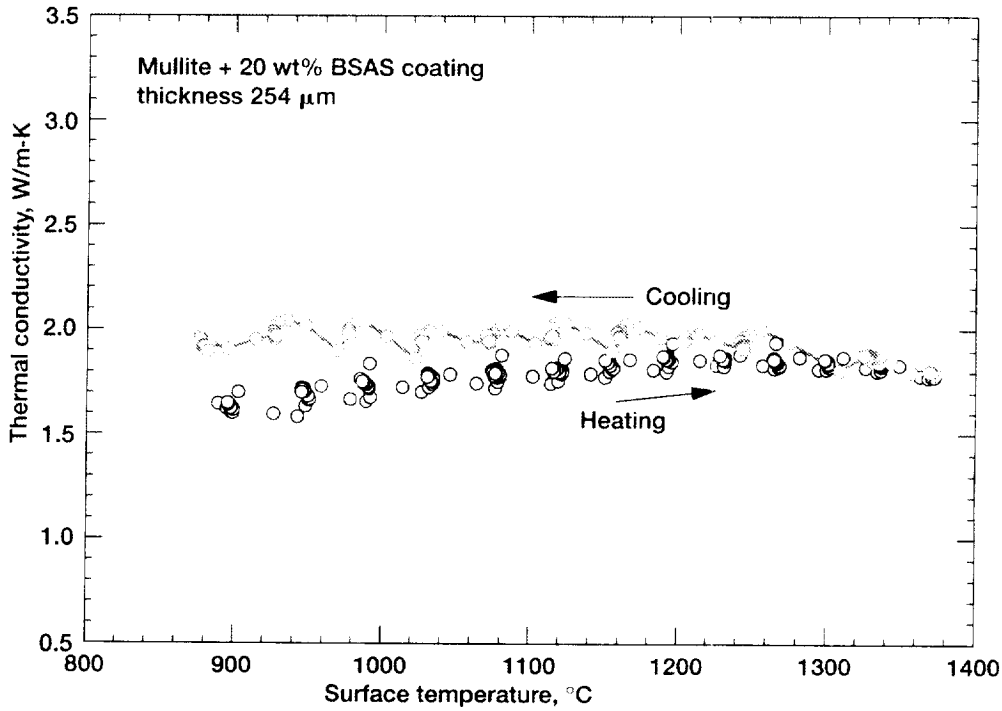

Figure 8.—Thermal conductivity of 254 μm thick mullite + 20 wt% BSAS coating on SiC/SiC CMC substrate as a function of test temperature. Thermal conductivity increase was observed during the heating/cooling cycle due to ceramic sintering.

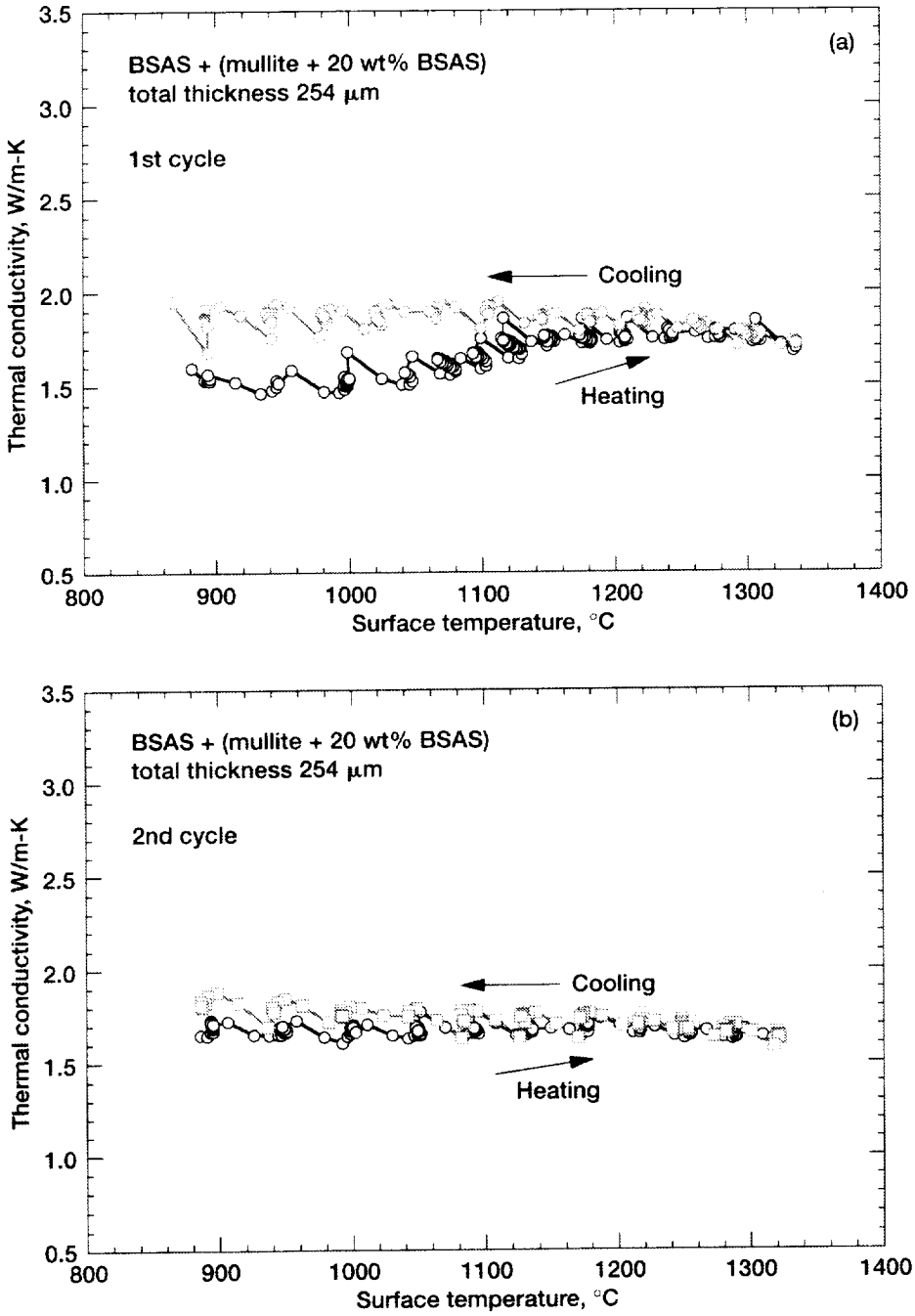

Figure 9.—Thermal conductivity of BSAS (127 μm thick)/mullite + 20 wt% BSAS (127 μm thick) on SiC/SiC CMC substrate as a function of coating test temperature. (a) The first heating-cooling cycle showed a larger conductivity increase due to ceramic sintering. (b) The second heating-cooling cycle had much less conductivity increase probably because most of the sintering and densification occurred during the first cycle.

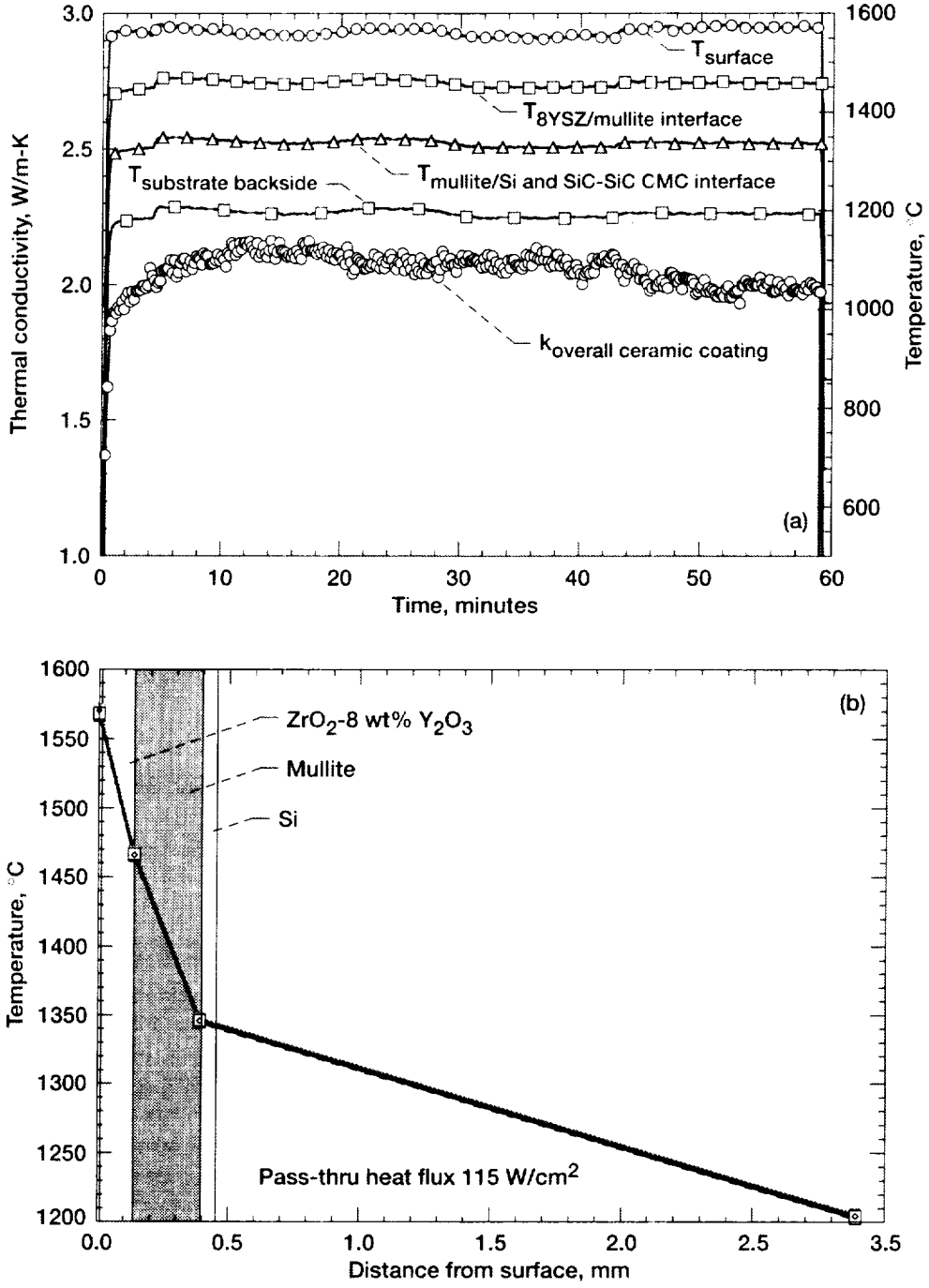

Figure 10.—Thermal conductivity of a ZrO_2-8 wt% Y_2O_3 (137μm)/mullite (254μm)/Si (76 μm) on a SiC/SiC CMC substrate. (a) Thermal conductivity increased during a short time high temperature exposure. (b) The estimated temperature distribution in the coating system.

REPORT DOCUMENTATION PAGE

Form Approved
OMB No. 0704-0188

1. AGENCY USE ONLY (Leave blank)	2. REPORT DATE	3. REPORT TYPE AND DATES COVERED
	September 2001	Technical Memorandum

4. TITLE AND SUBTITLE

Thermal Conductivity of Ceramic Thermal Barrier and Environmental Barrier Coating Materials

5. FUNDING NUMBERS

WU–714–04–20–00

6. AUTHOR(S)

Dongming Zhu, Narottam P. Bansal, Kang N. Lee, and Robert A. Miller

7. PERFORMING ORGANIZATION NAME(S) AND ADDRESS(ES)

National Aeronautics and Space Administration
John H. Glenn Research Center at Lewis Field
Cleveland, Ohio 44135–3191

8. PERFORMING ORGANIZATION REPORT NUMBER

E–12971

9. SPONSORING/MONITORING AGENCY NAME(S) AND ADDRESS(ES)

National Aeronautics and Space Administration
Washington, DC 20546–0001

10. SPONSORING/MONITORING AGENCY REPORT NUMBER

NASA TM—2001-211122

11. SUPPLEMENTARY NOTES

Dongming Zhu, Ohio Aerospace Institute, 22800 Cedar Point Road, Brook Park, Ohio 44142; Narottam P. Bansal and Robert A. Miller, NASA Glenn Research Center; Kang N. Lee, Cleveland State University, 1983 E. 24th Street, Cleveland, Ohio 44115–2403. Responsible person, Narottam P. Bansal, organization code 5130, 216–433–3855.

12a. DISTRIBUTION/AVAILABILITY STATEMENT

Unclassified - Unlimited
Subject Category: 27 Distribution: Nonstandard

Available electronically at http://gltrs.grc.nasa.gov/GLTRS

This publication is available from the NASA Center for AeroSpace Information, 301–621–0390.

12b. DISTRIBUTION CODE

13. ABSTRACT ***(Maximum 200 words)***

Thermal barrier and environmental barrier coatings (TBC's and EBC's) have been developed to protect metallic and Si-based ceramic components in gas turbine engines from high temperature attack. Zirconia-yttria based oxides and $(Ba,Sr)Al_2Si_2O_8$ (BSAS)/mullite based silicates have been used as the coating materials. In this study, thermal conductivity values of zirconia-yttria- and BSAS/mullite-based coating materials were determined at high temperatures using a steady-state laser heat flux technique. During the laser conductivity test, the specimen surface was heated by delivering uniformly distributed heat flux from a high power laser. One-dimensional steady-state heating was achieved by using thin disk specimen configuration (25.4 mm diam and 2 to 4 mm thickness) and the appropriate backside air-cooling. The temperature gradient across the specimen thickness was carefully measured by two surface and backside pyrometers. The thermal conductivity values were thus determined as a function of temperature based on the 1-D heat transfer equation. The radiation heat loss and laser absorption corrections of the materials were considered in the conductivity measurements. The effects of specimen porosity and sintering on measured conductivity values were also evaluated.

14. SUBJECT TERMS

Ceramic coatings; Thermal conductivity; Mullite; Zirconia; Celsian

15. NUMBER OF PAGES

21

16. PRICE CODE

17. SECURITY CLASSIFICATION OF REPORT	18. SECURITY CLASSIFICATION OF THIS PAGE	19. SECURITY CLASSIFICATION OF ABSTRACT	20. LIMITATION OF ABSTRACT
Unclassified	Unclassified	Unclassified	